

# Phase Changes in Embedded HMX in Response to Periodic Mechanical Excitation

Z. A. Roberts<sup>1,2,3</sup>, J. O. Mares<sup>2,4</sup>, J. K. Miller<sup>1,2,3,5</sup>, I. E. Gunduz<sup>1,2</sup>, S. F. Son<sup>1,2,4</sup>, and J. F. Rhoads<sup>1,3,5</sup>

<sup>1</sup> School of Mechanical Engineering

<sup>2</sup> Maurice J. Zucrow Laboratories

<sup>3</sup> Ray W. Herrick Laboratories

<sup>4</sup> School of Aeronautics and Astronautics

<sup>5</sup> Birck Nanotechnology Center

Purdue University

585 Purdue Mall, West Lafayette, IN 47907

## ABSTRACT

It is well known that energy can be spatially localized when explosives are mechanically deformed; however, the heat generation mechanisms associated with this localization process are not fully understood. In this work, mesoscale hot spot formation in ultrasonically-excited energetic materials has been imaged in real-time. More specifically, periodic, mechanical excitation has been applied to Dow Corning Sylgard® 184/octahydro-1,3,5,7-tetranitro-1,3,5,7-tetrazocine (HMX) composite materials using contact piezoelectric transducers resulting in heating at various crystal locations. A thermally-induced phase transition from a  $\beta$  to  $\delta$  non-centrosymmetric crystal structure for HMX results in the frequency doubling of incident laser radiation and can be used as a temperature proxy. In light of this, a high-repetition-rate 1064 nm Nd:YAG laser has been used to illuminate discrete HMX crystals, and a 532 nm filter has been applied to capture only the light emitted from  $\delta$ -phase second harmonic generation (SHG). The visualization of  $\delta$ -phase initiation and growth is useful for determining both heat generation mechanisms and heating rates at crystal/crystal and/or crystal/binder interfaces and contributes to the understanding and prediction of hot spots.

## KEYWORDS

Ultrasonics, Hot spots, Second harmonic generation, Composite explosives, Energetic materials

## 1. INTRODUCTION

The initiation of explosives, and in particular polymer-bonded explosives (PBXs), is often attributed to *hot spots*, which form due to intense energy localization resulting from mechanical dissipation and/or adiabatic heating [1,2]. Hot spots are inherently difficult to observe and characterize due to their transient nature. Particular hurdles involve taking measurements at extremely high temperatures and pressures, and making observations at very small timescales and spatial locations. Recently, hot spots have been observed (using infrared imaging) in energetic systems that were excited via high-frequency, ultrasonic excitation [3-6]. Such excitation appears to be useful for improving the understanding of hot spot generation at longer timescales than those commonly seen in short-duration shock events. Non-intrusive temperature indicators would be helpful in such experiments as they can help validate infrared thermography measurements.

The explosive octahydro-1,3,5,7-tetranitro-1,3,5,7-tetrazocine (HMX) is used in composite PBXs, typically as energetic crystals which are embedded in a polymer binder, commonly hydroxyl-terminated polybutadiene (HTPB) or Estane® 5703 [7-10]. At room temperature, the most stable and dense polymorph of HMX is the  $\beta$ -phase [7].  $\beta$ -HMX crystals transform from a centrosymmetric to a non-centrosymmetric  $\delta$ -phase when heated above  $\sim 170$  °C. A laser source can interfacially or volumetrically generate frequency doubled light because of the nonlinear optical properties of the  $\delta$ -phase crystal [11-14]. This was first observed for HMX by Henson *et al.* [12] and has since been successfully used in a number of studies as a  $\delta$ -phase indicator [8,15,16]. The use of second harmonic generation (SHG) may provide new time-resolved information of the state of individual energetic crystals. As an *in situ* imaging technique implemented during ultrasonic experiments, SHG serves as an indirect temperature marker capable of observing the localization of energy in energetic crystals.

While SHG techniques have been used in dropweight experiments of  $\delta$ -HMX containing materials [15,16], they are yet to be used to investigate the interaction among various explosive crystals and/or any surrounding binder material, which may be

key component of hot spot generation [1]. Given the crucial need to investigate possible frictional or viscoelastic heating mechanisms at crystal/crystal and/or crystal/binder interfaces for PBX munitions undergoing mechanical deformation, this work seeks to observe how hot spots created by ultrasonic excitation affect crystals embedded within a binder and to verify infrared thermography measurements via the indirect temperature markers of both phase change and decomposition.

It was noted in prior work that individual crystals should have no geometric features, such as cracks or microinclusions, whereat initial phase change nucleation can be specifically pinpointed [7,8]. As such, care should be taken when drawing conclusions about hot spot locations from SHG origination on a single crystal. However, it is possible to better understand the underlying physics of an experiment from the observation of crystal phase transitions when considering the inclusion positions and duration of excitation.

## 2. EXPERIMENTAL DESIGN

Wet, Grade B, Class 3  $\beta$ -HMX crystals manufactured by BAE Systems (lot BAE13E071-132) were selected as inclusions in the composite samples. The HMX was sieved to be greater than 425  $\mu\text{m}$  to avoid influences of crystal size on the SHG signal [3,7,11]. In addition to being easily visible in the binder, coarser HMX crystals have the additional benefit of tending to phase transition at a lower temperature than finer crystals [11]. Samples included four HMX crystals carefully arranged to be in close proximity and lying on the same plane within a Dow Corning Sylgard® 184 silicone elastomer. Crystal proximity is an important factor in dropweight sensitivity testing [1], and for this reason, a system of multiple crystals was selected for this study. One of the four crystals in each sample was prepared as  $\delta$ -phase for ease of laser alignment and focusing on the SHG signal [16]. It also served as a point of reference and comparison in optical microscope images.  $\delta$ -HMX was created from the sieved  $\beta$ -HMX by heating the crystals on a plate at approximately 200  $^{\circ}\text{C}$  for several minutes until the crystals visibly changed to an opaque white color and increased in size. A 7% volume increase from  $\beta$  to  $\delta$ -phase is noted by several authors [11,15] when creating  $\delta$ -HMX by different heating procedures. This phenomenon was clearly observed throughout the course of the experiment described herein.  $\delta$ -HMX was cast into the Sylgard within a day, and tests were performed within four weeks to avoid possible reversion to  $\beta$ -phase or an alternate phase. Smilowitz *et al.* noticed that  $\delta$ -HMX spontaneously transformed to  $\alpha$ -HMX at room temperature after a time [8], and Czerski *et al.* expressed similar concerns [15].

Sylgard has been used in PBXs and was chosen as the binding material in this study due to its optical transparency at both the visible and near-infrared wavelengths. All samples were cast simultaneously in Sylgard at a 10:1 wt. ratio of base to curing agent. As in prior work [3,5], to facilitate the embedding of discrete crystals, multiple casting and curing steps were performed. At each casting step, liquid Sylgard was degassed under vacuum and then cured at 65  $^{\circ}\text{C}$  for 12 hours [6,7,9,10,17]. First, a ‘base layer’ of  $1\pm 0.2$  mm was cast and cured. HMX crystals were then placed onto the base layer and totally encapsulated in a secondary layer of Sylgard. Finally, small rectangular sections were cut from this composite with a razor blade and placed into a variable-height mold with exterior dimensions of 6.6 x 8.9 mm. Each mold was then filled with binder to two different heights: 4.5 mm (short) and 8.1 mm (tall). Figure 1 presents a dimensioned illustration of a single-particle short sample. All samples were tested within four weeks of manufacture to avoid stiffening from aging [17].

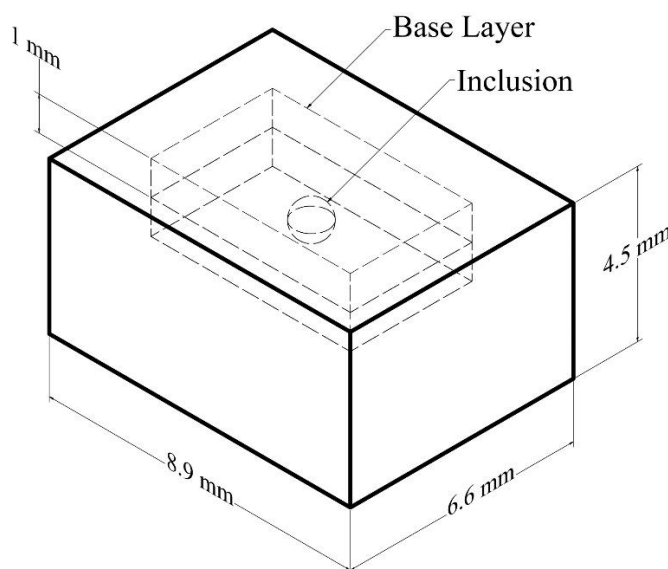


**Fig. 1** An illustration of the final dimensions and casting steps of a short sample

A Steiner & Martins, Inc. SMD10T2R111 piezoelectric, ultrasonic transducer which has a nominal resonant frequency of 215 kHz was selected to conform to previous works [3]. As seen in Figure 2, each sample was attached to a transducer with Devcon Flow-Mix 5 Minute® epoxy and allowed to cure at room temperature. It was determined from the infrared imaging of a soot coated sample that a frequency of 210.5 kHz achieved the highest temperature increase for the system. A sinusoidal signal was sent to the transducer with a Keysight Technologies N9310A RF Signal Generator at -3.0 dBm. In combination with a Mini-Circuits LZY-22+ High Power Amplifier, this supplied an on-sample power level of 10 W for a duration of approximately 20 s.

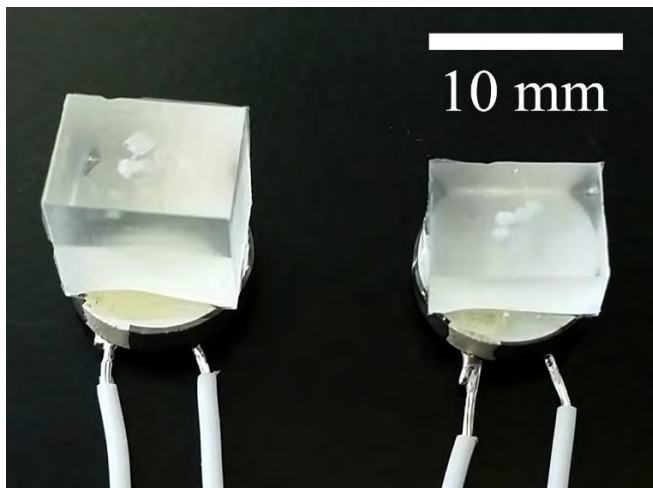


**Fig. 2** Representative tall (left) and short (right) samples attached to the piezoelectric transducers

HMX crystals within the Sylgard sample were illuminated by a 1064 nm wavelength Nd:YAG laser with a pulse repetition frequency of 40 kHz. After beam expansion, the power was measured to be 5.6 W with a  $1/e^2$  diameter of 1.5 mm. Because the influence of laser heating was a concern [15], the power level and diameter were chosen as the minimum values required for an easily-observable SHG signal capable of illuminating all four crystals. This was a lower power and smaller spot size than the lasers reportedly used in other SHG works [12,15,16]. The laser alone was verified to be insufficient to cause phase change at these timescales and the beam passed directly from the side through the Sylgard block without being incident on the transducer.

Images capturing SHG light were taken at 30 frames per second with a Canon XL2 3CCD MiniDV Camcorder on a low-light setting with an EF 100 mm f/2.8 macro lens. A 532 nm notch filter was inserted between the camera and the illuminated sample, as shown in Figure 3. Experiments were conducted in a darkened room to ensure that the only light reaching the camera would be from the SHG at 532 nm.

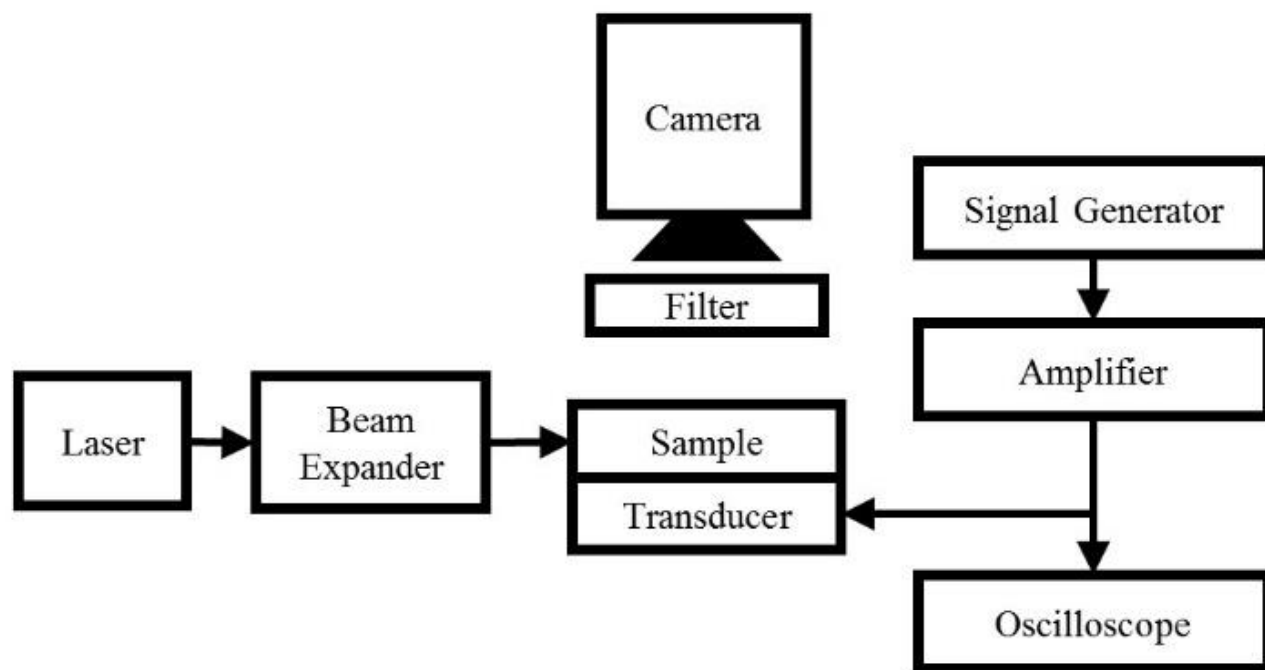


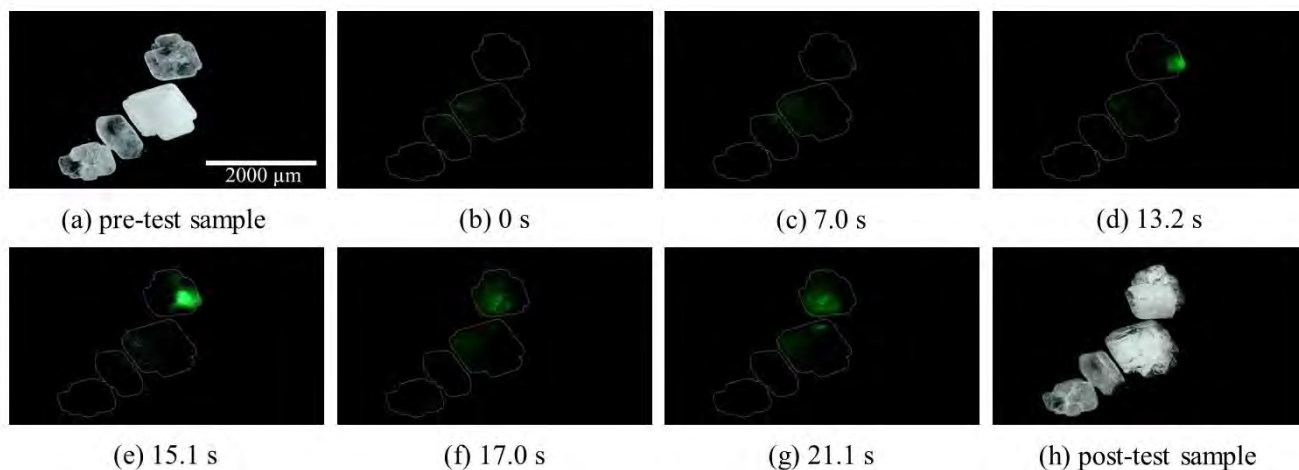
**Fig. 3** Schematic showing the relative positions of the camera and laser

The camera could detect and register some near-infrared radiation, and so prior to each test, the laser was aligned without the 532 nm filter in place. This ensured that the beam illuminated all of the crystals within the Sylgard block. After alignment, the environment was darkened after several minutes and the trial began. Excitation time was monitored with an oscilloscope, and if SHG light was seen before  $\sim 10$  s, the individual trial was allowed to continue for additional time up to approximately 20 s. The laser gate was opened approximately one second before the test began so that its contribution to heating was minimized. ‘Pre-test’ and ‘post-test’ images were taken with a Hirox KH-8700 digital microscope.

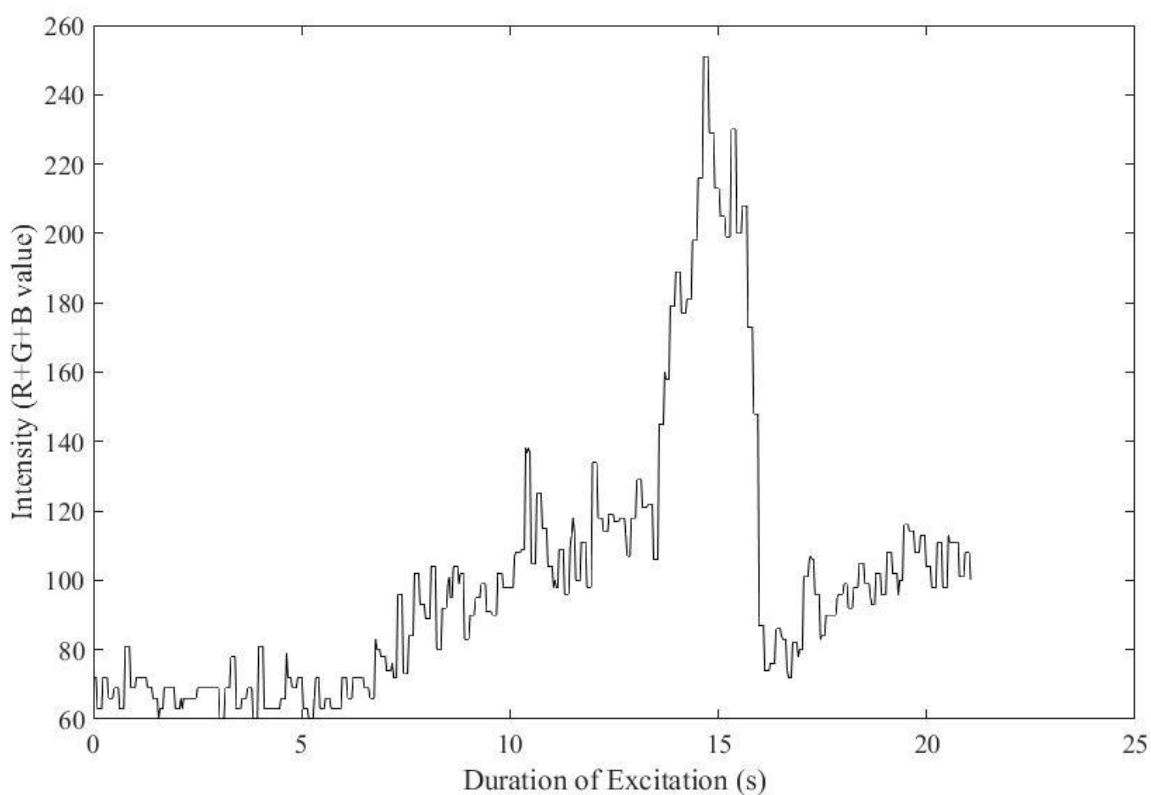
### 3. RESULTS

In Figures 4, 6 and 7, real-time observations of the dynamic phase change of individual HMX crystals in a Sylgard binder are presented. The samples were illuminated by 1064 nm wavelength radiation from the left and some shadowing effects of the frequency doubled 532 nm light were present when phase changes occurred. Radiation may have been blocked by some  $\delta$  phase-changing crystals that scatter light significantly. Consequently, in some samples, green SHG light was not sustained. In Figures 4, 6 and 7, frame (b) corresponds to 0 s, which is defined as the time at which the transducer was powered. Frame (c) corresponds to the first SHG emission, which varied from 6.9 s to 10.6 s. Note that the captured SHG light contrast and saturation have been enhanced here, and an outline has been added in these stills around individual crystals so that the SHG is more easily seen. Frame (g) corresponds to the termination of each test, after which both the transducer and laser were turned off. All video frames presented are from the results of the ultrasonic excitation of the short samples. For all cases involving the tall samples, except for one which received over 20 s of excitation, the induced heating was insufficient to result in a phase transition of the embedded crystals.

In the first example, the uppermost crystal in Figure 4(c) emitted initial SHG light. The highly-reflected green light proceeded to grow in intensity and propagate leftward across the crystal over the next few seconds. Figure 4(e) captured the most intense reflection of SHG light. The SHG signal at the point of maximum intensity on the upper crystal is shown versus time in Figure 5. As observed in Figure 4(h), the uppermost crystal has a cracked and opaque appearance. It also appears to have noticeably increased in volume as should be expected for  $\delta$ -phase HMX [11,13,15]. The lower crystals in the figure have not changed significantly.

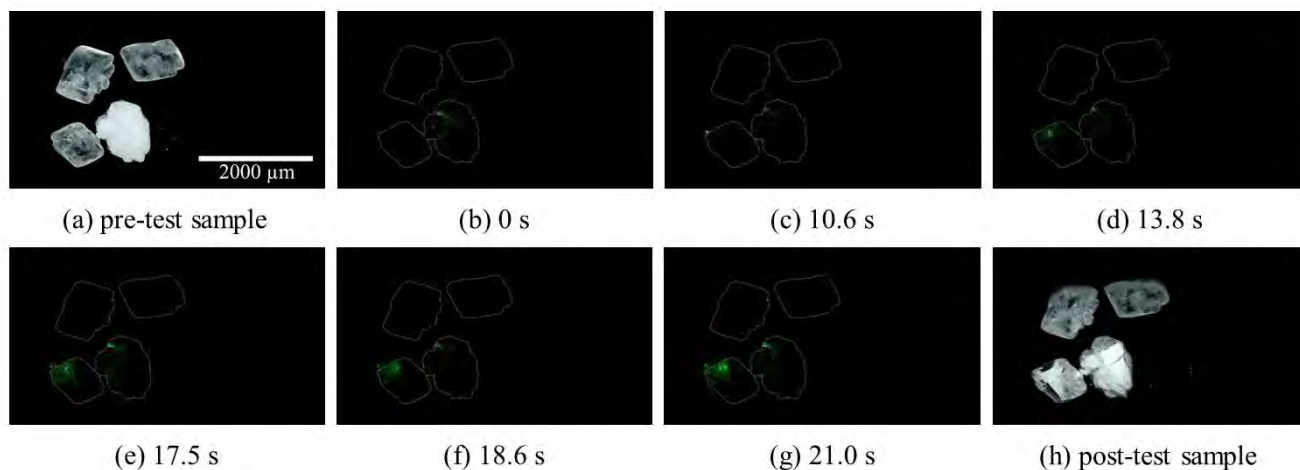


**Fig. 4** Selected frames showing a high reflectance of SHG green light during propagation across one of the embedded  $\beta$ -HMX crystals



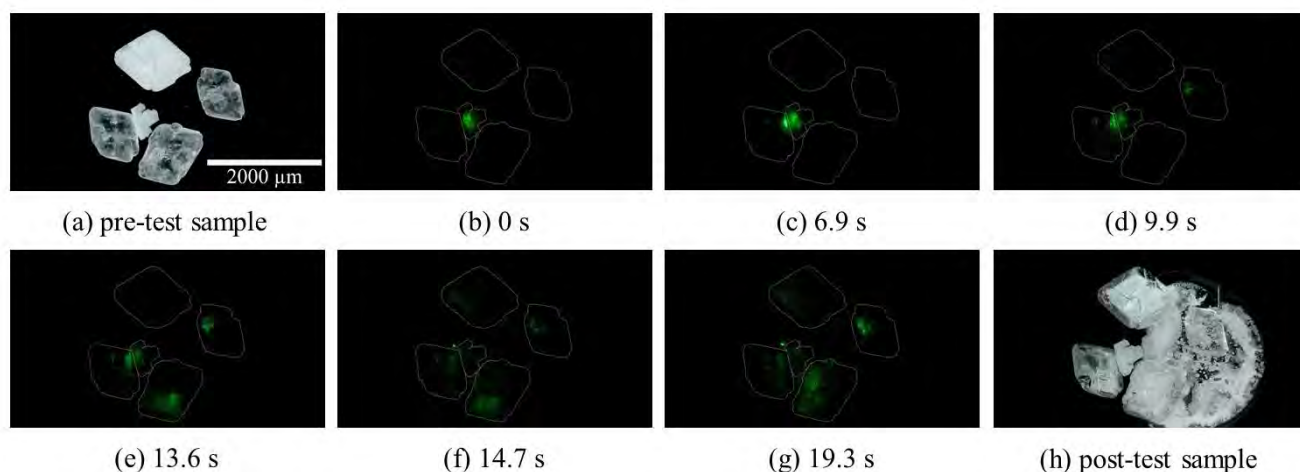
**Fig. 5** Plot of intensity versus excitation time at the point of maximum observed SHG

Figure 6 illustrates another instance of a single crystal undergoing phase transformation. This was the typical case in these experiments wherein not all of the crystals changed phase even after 21.0 s of excitation. At time 0 s, SHG green light from the  $\delta$ -HMX inclusion in Figure 6(b) is reflected off of the left side of the crystal. Additional SHG light began in Figure 6(c) with a bright point suddenly appearing on the smaller, lower-left crystal. This point dimmed while the rest of the crystal slowly faded to green in Figure 6(d), and was followed by the bright point reappearing in Figure 6(e).



**Fig. 6** Selected frames showing a representative SHG response of a single-crystal transition event

A sample that underwent a decomposition event is presented in Figure 7. Additional SHG light was first seen after 6.9 s in Figure 7(c) located where an adjacent  $\delta$ -HMX crystal fragment was in contact with the original  $\beta$ -HMX. This began with bright interfacially-generated green light. All of the crystals in the binder experienced a phase transition in this trial. After 14.7 s, in Figure 7(f), the sample visibly shifted under the camera. This was due to the sudden decomposition of HMX in which a gas pocket subsequently burst open the binder in the plane that was formed during casting as shown in Figure 7(h).



**Fig. 7** Selected frames showing SHG response of embedded HMX crystals which resulted in decomposition

Of the nine short samples tested, examination of the post-test microscope images revealed additional  $\delta$ -HMX in all but one sample. Not all of the  $\delta$ -HMX crystals demonstrated SHG, most likely due to a combination of shadowing effects or an insufficient irradiance near the edge of the beam. In four of the eight samples that experienced a phase transition, only a single crystal changed, while the other four samples experienced multiple phase-changed crystals. Three samples with multiple phase-changed crystals decomposed, two of which broke the surface of the Sylgard layer resulting in a low, but audible report.

#### 4. DISCUSSION AND CONCLUSIONS

In this work, SHG of HMX crystals in a binder under ultrasonic stimulation has been shown to provide a real-time indication of the crystal phase and was therefore used as a temperature marker. For the experimental configuration presented in this work, different mechanisms may be responsible for heating. In the near-field of the transducer, and around inclusions, there are expected to be non-uniform stresses and deformations in the plane of interest. These areas of concentrated stresses could be considered hot spots with points of intense heating. This heating would raise the temperature of the nearby HMX crystals resulting in a phase change once they reached 170 °C. Other crystals in the binder are expected to have lower temperatures than 170 °C when SHG light is initially detected.

Surface asperities, crystals in close proximity, as well as points of contact between crystals may be responsible for localized frictional or viscoelastic heating as passing waves induce stress in the binder [2,5,18]. Mechanical energy dissipated in this way may also induce delamination at the crystal/binder interface resulting in increased frictional effects. SHG results akin to those presented in this work seem to indicate  $\delta$ -phase propagation from interfaces. Smilowitz *et al.* suggests that SHG light observed from nucleation sites cannot be associated with crystal morphology or defects [8]; however, their experiment explored uniform heating over hours and does not address how a rapidly-deforming binder would interact with crystal features.

There were results presented in this work in which a single HMX crystal experienced SHG, regardless of the size of the other crystals in the same binder. There were also long periods of excitation after an initial phase change during which no other crystals transitioned. Using the results from Saw [11], which show that larger HMX crystals change phase first, one can interpret single-crystal transitions as being indicative of hot spots formed from focused acoustic energy. The smaller individual crystal was likely near a point of high stress concentration in the near-field of the transducer, while the others were not. This experimental technique is limited by the fact that the HMX inclusions must reach temperatures on the order of 170 °C. This fact was expounded in the taller samples where crystals located farther away from the near-field effects of the transducer did not experience any phase change. Given the combined effects of being further away from the near-field and resistive heating, no temperature information was gained from the HMX crystals in the tall samples. Conclusions cannot necessarily be drawn from where the SHG began to occur on, or in, individual crystals [8,13], but this work has shown that the transitioning crystals are an indication of hot spot locations.

The acoustic insult of composite energetic particle and elastic binder systems in similar configurations [3] have been shown to drive ammonium perchlorate (AP) and HMX crystals to decomposition. In the present work, the decomposition of HMX crystals is indicative of reaching 290 °C [11] after which on a hotplate the crystals would normally form an amorphous structure and burn. In the work of Mares *et al.* [3], infrared thermography has quantified the radiation emitted from the surface of similar composites, but failed to capture the exact temperature at hot spot locations. The technique of SHG employed herein has provided more information about particle temperatures within the binder and has shown that the inclusions are capable of reaching 170 °C and above. Mares *et al.* reported observing a maximum surface temperature rise over 2 s of excitation of 57.93 °C with an estimated HMX particle temperature of 74.24 °C [3]. This is consistent with the ~20 °C/s temperature rise obtained using the SHG results presented in the current work. You *et al.* reported a hot spot temperature for polyethylene glycol (PEG) coated sucrose in a polydimethylsiloxane (Sylgard 182) binder which reached ~327 °C with a reported 22,000 °C/s heating rate and approached the dynamic range limit of their camera [6]. While this is curiously above the melting temperature of sucrose, it is in the range of HMX decomposition temperature indicated in the current work with low-power excitation.

Future work should address how the heating mechanisms associated with acoustic interactions compare to that in shock and impact studies. Additionally, future work should focus on the effect of crystal proximity and the time to initial SHG. Investigations should examine how energy deposited from passing acoustic waves affects the rate of heating and SHG kinetics over time [13]. SHG should also be used to validate temperature measurements of encapsulated crystals. Others have shown that the  $\delta$ -phase transition may be a precursor, or linked, to ignition [15], and therefore the phase transition phenomenon is an important consideration in munitions subjected to shock, vibration, and heating.

## 5. ACKNOWLEDGEMENTS

This work was made possible by support from the U. S. Air Force Office of Scientific Research through award no. FA9550-15-1-0102 and the project's Program Manager Dr. Jennifer Jordan. The author J. O. Mares would like to express gratitude to the National Science Foundation Graduate Research Fellowship Program under grant no. DGE-1333468.

## 6. REFERENCES

- [1] Y. Q. Wu & F. L. Huang, Experimental investigations on a layer of HMX explosive crystals in response to drop-weight impact, *Combust. Sci. Technol.* **185:2**, 269-292, 2013.
- [2] J. E. Field, Hot spot ignition mechanisms for explosives, *Accounts Chem. Res.* **25:11**, 489-496, 1992.
- [3] J. O. Mares, J. K. Miller, I. E. Gunduz, J. F. Rhoads & S. F. Son Heat generation in an elastic binder system with embedded discrete energetic particles due to high-frequency, periodic mechanical excitation, *J. Appl. Phys.* **116:20**, 204902, 2014.

- [4] J. O. Mares, J. K. Miller, N. D. Sharp, D. S. Moore, D. E. Adams, L. J. Groven, J. F. Rhoads & S. F. Son, Thermal and mechanical response of PBX 9501 under contact excitation, *J. Appl. Phys.* **113:8**, 084904, 2013.
- [5] J. K. Miller, J. O. Mares, I. E. Gunduz, S. F. Son & J. F. Rhoads, The impact of crystal morphology on the thermal responses of ultrasonically-excited energetic materials, *J. Appl. Phys.* **119:2**, 024903, 2016.
- [6] S. You, M. Chen, D. D. Dlott & K. S. Suslick, Ultrasonic hammer produces hot spots in solids, *Nat. Commun.* **6**, 6581, 2015.
- [7] A. E. D. M. van der Heijden & R. H. B. Bouma, Crystallization and characterization of RDX, HMX and CL-20, *Cryst. Growth Design* **4:5**, 999–1007, 2004.
- [8] L. Smilowitz, B. F. Henson, M. Greenfield, A. Sas, B. W. Asay & P. M. Dickson, On the nucleation mechanism of the  $\beta$ - $\delta$  phase transition in the energetic nitramine octahydro-1,3,5,7-tetranitro-1,3,5,7-tetrazocine, *J. Chem. Phys.* **121:11**, 5550-5552, 2004.
- [9] M. A. Daniel, Polyurethane binder systems for polymer bonded explosives, *DSTO-GD-0492*, 2006.
- [10] B. L. Hamshere, I. J. Lochert & R. M. Dexter, Evaluation of PBXN-109: the explosive fill for the penguin anti-ship missile warhead, *DSTO-TR-1471*, 2003.
- [11] C. K. Saw, Kinetics of HMX and phase transitions: effects of particle size at elevated temperature, *Proc. 12th Int. Det. Symp.* 70-76, 2002.
- [12] B. F. Henson, B. W. Asay, R. K. Sander, S. F. Son, J. M. Robinson, P. M. Dickson, Dynamic measurement of the HMX  $\beta$ - $\delta$  phase transition by second harmonic generation, *Phys. Rev. Lett.* **82:6**, 1213–1216, 1999.
- [13] L. Smilowitz, B. F. Henson, B. W. Asay & P. M. Dickson, The  $\beta$ - $\delta$  phase transition in the energetic nitramine octahydro-1,3,5,7-tetranitro-1,3,5,7-tetrazocine: kinetics, *J. Chem. Phys.* **117:8**, 3789-3798, 2002.
- [14] F. Simon, S. Clevers, V. Dupray & G. Coquerel, Relevance of the second harmonic generation to characterize crystalline samples, *Chem. Eng. Technol.* **38:6**, 971-983, 2015.
- [15] H. Czerski, W. L. Perry & P. M. Dickson, Solid state phase change in HMX during dropweight impact, *Proc. 13th Int. Det. Symp.* 681-688, 2007.
- [16] H. Czerski, M. W. Greenaway, W. G. Proud & J. E. Field,  $\beta$ - $\delta$  Phase transition during dropweight impact of cyclotetramethylene-tetranitroamine, *J. Appl. Phys.* **96:8**, 4131-4134, 2004.
- [17] V. Placet & P. Delobelle, Mechanical properties of bulk polydimethylsiloxane for microfluidics over a large range of frequencies and aging times, *J. Micromech. Microeng.* **25:3**, 035009, 2015.
- [18] F. P. Bowden & A. D. Yoffe, Initiation and growth of explosion in liquids and solids, *Cambr. Univ. Press*, 1952.